


RESEARCH PAPER

 OPEN ACCESS

Fabrication and surface modification of poly lactic acid (PLA) scaffolds with epidermal growth factor for neural tissue engineering

Tanit Haddad^a, Samantha Noel^a, Benoît Liberelle^a, Rouwayda El Ayoubi^b, Abdellah Ajji^a, and Gregory De Crescenzo ^a

^aDepartment of Chemical Engineering, École Polytechnique de Montréal, Centre-Ville, Montréal (QC), Canada; ^bNew World Laboratories Inc., Laval (QC), Canada

ABSTRACT

In an effort to design biomaterials that may promote repair of the central nervous system, 3-dimensional scaffolds made of electrospun poly lactic acid nanofibers with interconnected pores were fabricated. These scaffolds were functionalized with polyallylamine to introduce amine groups by wet chemistry. Experimental conditions of the amination protocol were thoroughly studied and selected to introduce a high amount of amine group while preserving the mechanical and structural properties of the scaffold. Subsequent covalent grafting of epidermal growth factor was then performed to further tailor these aminated structures. The scaffolds were then tested for their ability to support Neural Stem-Like Cells (NSLCs) culture. Of interest, NSLCs were able to proliferate on these EGF-grafted substrates and remained viable up to 14 d even in the absence of soluble growth factors in the medium.

ARTICLE HISTORY

Received 3 August 2015
Revised 22 March 2016
Accepted 26 August 2016

KEYWORDS

adhesion; amine functionalization; cell proliferation; electrospinning; epidermal growth factor grafting; poly lactic acid




Introduction

While intrinsic healing of the central nervous system (CNS) after injuries is very limited, recent progress within the field of stem cell therapy has opened new and promising avenues. The use of human neural stem / progenitor cells (NS/PC) has attracted a lot of interest since these cells can be easily expanded while their neural lineage is inherently specified. Their use led to extremely promising results in animal models.¹⁻³ For optimal results, stem cell delivery may be combined to scaffold design and biomolecule delivery in order to bolster regeneration.

The use of NS/PC requires their selective expansion, a process that involves specific growth factors (*i.e.*, the epidermal and fibroblast growth factors, EGF and FGF, respectively).^{4,5} Accordingly, in many studies, the implantation of NS/PC has been accompanied with concomitant infusion of specific proteins to promote cell survival, proliferation and differentiation^{6,7} as well as to increase axonal regeneration.⁸ One alternative strategy relies on protein inclusion within appropriate structures made of biodegradable and biocompatible

polymeric materials.⁸⁻¹⁰ The objective is to control their spatiotemporal delivery to damaged regions of the CNS, while physically guiding regeneration. For that purpose, several hydrogels have been tested, including those made of agarose, alginate, methylcellulose, dextran and chitosan as well as polysaccharide blends. Hydrogels present many advantages for neural tissue regeneration, including the ability to deliver growth factors or other biological cues.¹¹ Soft, positively charged surfaces as those obtained with dextran/chitosan blends were also reported to favor neuron attachment.¹² Hyaluronic acid (HA) was also shown to offer adequate mechanical support as well as good cell adhesion, proliferation and migration properties.¹³

Of interest, as an alternative to hydrogels, electrospinning has been investigated for neural regeneration as the generation of 3-dimensional scaffolds made of micro- to nano- size fibers with controlled properties may be of great potential for cell differentiation and neurite outgrowth.^{14,15} Indeed, electrospun scaffolds, including those made of poly lactic acid (PLA), are highly porous and their topography mimics the

CONTACT Gregory De Crescenzo  gregory.decrescenzo@polymtl.ca; Abdellah Ajji  abdellah.ajji@polymtl.ca  École Polytechnique de Montréal, P.O. Box 6079 Station, Centre-ville, Montreal (QC), H3C 3A7 Canada

© 2016 Tanit Haddad, Samantha Noel, Benoît Liberelle, Rouwayda El Ayoubi, Abdellah Ajji, and Gregory De Crescenzo. Published with license by Taylor & Francis.

This is an Open Access article distributed under the terms of the Creative Commons Attribution-Non-Commercial License (<http://creativecommons.org/licenses/by-nc/3.0/>), which permits unrestricted non-commercial use, distribution, and reproduction in any medium, provided the original work is properly cited. The moral rights of the named author(s) have been asserted.

natural extracellular matrix (ECM), which makes them good candidates for neural tissue engineering.^{16,17} However, polyester surfaces are characterized by a suboptimal hydrophilicity for cell adhesion, which may limit their use unless functional groups or molecules promoting cell attachment are introduced. Surface modification such as the aminolysis technique has been widely used for the addition of amine groups in order to covalently bind bioactive molecule.^{18,19}

This study aims to fabricate PLA nanofibers by electrospinning to be used as neural tissue engineering scaffolds. The PLA scaffolds were functionalized with amine groups via a novel aminolysis treatment using polyallylamine (PAAm).^{20,21} The prepared scaffolds were characterized by scanning electron microscopy (SEM) and amine moieties were quantified using the Orange II method.²² EGF was then tethered onto the PLA electrospun scaffolds. In this study, we have used *in vitro* engineered Neural Stem Like-Cells derived from skin cells by direct reprogramming using a defined transcription factor.²³ These cells have the ability to self renew, they are identical to neural stem cells in morphology, gene and protein expression profile, and even *in vitro* and *in vivo* functionality. The impact of the EGF-grafted PLA nanofiber scaffolds upon NSLC adhesion, survival and proliferation was then evaluated, with the ultimate goal of developing an improved strategy for neural tissue engineering.

Results

Aminolysis of PLA nanofibers

PLA nanofibers mats were electrospun as described in the materials and methods section, allowing for the creation of 3D scaffolds with interconnected pores, made of randomly oriented fibers (see SEM images of pristine mats, Fig. 2A). The average fiber diameter of the nanofibers was 408 ± 77 nm with a fiber mat of about 87% porosity (Table 1, condition A). Amine functionalization of the electrospun PLA nanofibers was performed using 2 aminated polymers, polyallylamine (PAAm, 15 kDa) and polyvinylamine (PVAm, 25 kDa) as well as a short diamine molecule, *i.e.*, ethylenediamine (EtDA). In each case, covalent amide bonds were formed between the PLA and the amine-containing (macro)-molecules, as presented in Figure 1.

Interestingly, all of the aminolysis conditions we tested had little effect on the porosity values when

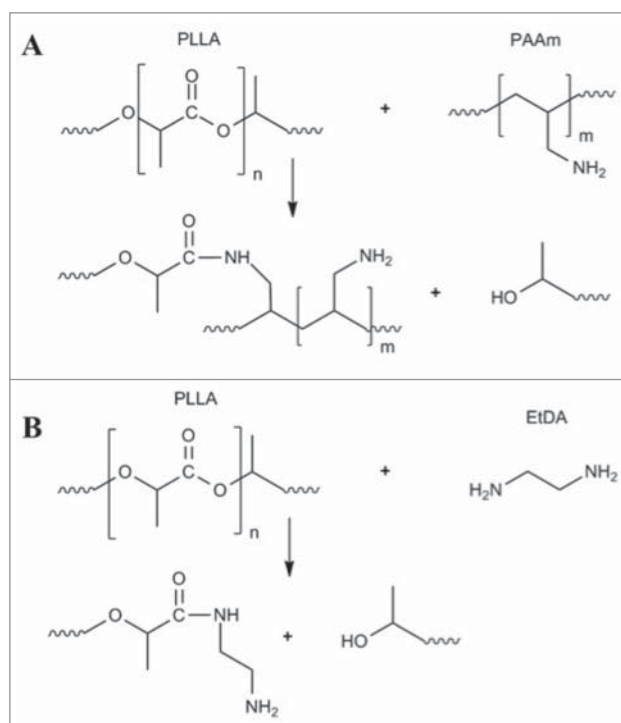


Figure 1. PLA aminolysis reaction involving (A) polyallylamine (PAAm) and (B) ethylenediamine (EtDA).

compared to untreated samples (85% after aminolysis, and about 87% for pristine mats, Table 1). Similarly, the average fiber diameter after any of the treatment was close to the values obtained for pristine mats (443 ± 28 and 408 ± 77 nm, respectively). Amine groups were successfully added to the PLA fibers using PAAm (Table 1, conditions B–F). A significant increase in amine density, up to about $100 \mu\text{mol/g}$, was observed when compared to the control samples (condition H: pristine samples immersed in water and dioxane). PAAm-based aminolysis was performed on the PLA samples for 1, 3, and 20 h at 60°C and pH 12.5 (condition B, C and D, respectively; Table 1 and Fig. 2). Although some fibers appeared to break or degrade based on the SEM images (Fig. 2D), the average fiber diameter (AFD) remained the same as seen in the pristine mat. A complete dissolution of the PLA nanofibers was observed for a reaction time of 24 h (data not shown). No significant change in amine group density was noticed for reaction time ranging from 1 to 3 h (conditions B vs C, Table 1). PAAm-based aminolysis was also performed at a temperature lower than the T_g of the PLA (*ca.* 57°C)²⁴, with no influence on the surface amine group quantity or AFD (conditions B vs F, Table 1). However, when the pH of the reaction was adjusted to 11.5 (condition E, Table 1), a significant

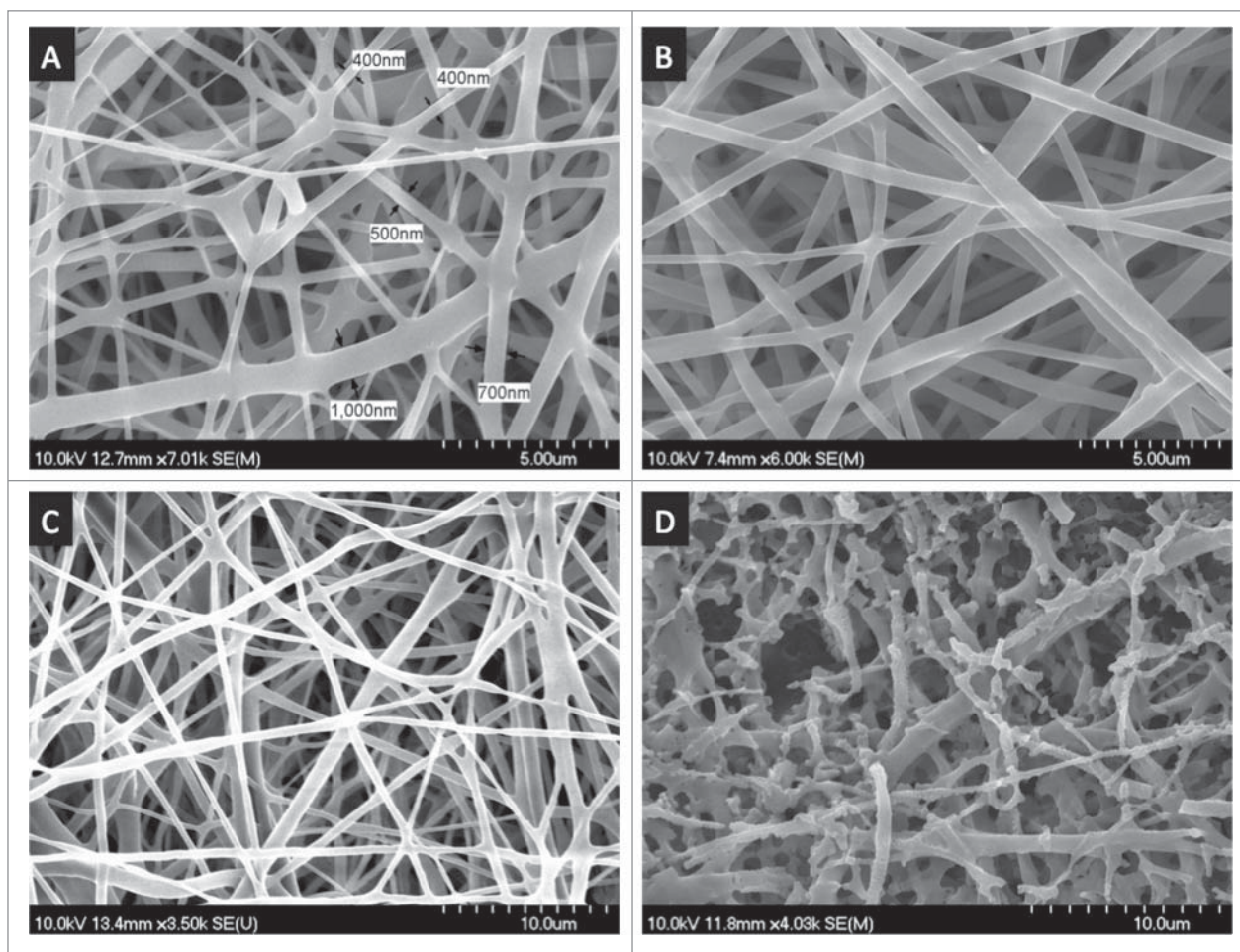


Figure 2. SEM imaging of (A) pristine and (B-D) PAAm-treated PLA nanofibers. PAAm grafting was carried out at pH 12.5 and 60°C for (B) 1 h, (C) 3 h, and (D) 20 h.

decrease in amine group density was observed compared to a pH of 12.5 (condition F, Table 1). Altogether, the density of exposed amine groups via a polymer-based aminolysis appeared to be mainly guided by the pH of the reaction mixture, as previously observed for PET films²² and PET fibers.²¹ No significant difference in weight was observed before and after aminolysis for any of the conditions (except for conditions for which degradation was observed).

Accordingly, condition F, *i.e.*, 50°C and pH 12.5 for 1 h, was selected as the optimal one for PAAm-based aminolysis, as it provided the highest amino group density ($133.2 \pm 16.3 \mu\text{mol/g}$) with no significant impact on AFD and mat porosity compared to the pristine mat (condition A, Table 1). A 50°C reaction temperature was also selected as one may not expect any drastic fiber deformation below the T_g temperature. Furthermore, mechanical testing of these mats revealed that no significant difference can be observed between control samples (in water and dioxane) and

PAAm-reacted samples (condition F, Table 1). Indeed, the Young's modulus values of the dry mat, of the mat in wet conditions prior and after aminolysis were of 70, 45 and 35 MPa, respectively. The decrease of the Young's modulus of the pristine mats after they had been placed in wet conditions was probably due to hydration as water acts as a plasticizer.^{25,26} A more complete study on the evolution of mat morphology with process and material parameters will be published elsewhere (manuscript in preparation).

For the sake of comparison, aminolysis was also performed using PVAm and EtDA. Under the optimized conditions for PAAm, the PVAm (condition G, Table 1) was found to be less efficient to introduce amino groups in the PLA nanofibers ($76.68 \pm 9.84 \mu\text{mol/g}$) without affecting the AFD. In contrast, when the small EtDA molecule was reacted with PLA mats (conditions J-L, Table 1), the resulting amino group density remained low (*ca.* $0.4 \pm 0.1 \mu\text{mol/g}$) for reaction time varying from 10 to 30 min and was

Table 1. Properties of pristine and aminolysed PLA nanofibers.

	Treatment	pH	Reaction time	Reaction temperature (°C)	Average Fiber Diameter (AFD, nm, $n = 10$)	Porosity (% , $n = 3$)	Amine group density ($\mu\text{mol/g}$, $n = 3$)
A	Pristine				408 ± 77	87	
B		12.5	1 h	60	407 ± 62	N/D	109.8 ± 23.7
C		12.5	3 h	60	474 ± 69	N/D	120.3 ± 26.3
D	PAAm	12.5	20 h	60	461 ± 94	N/D	N/A
E		11.5	1 h	50	465 ± 114	89	88.6 ± 22.7
F		12.5	1 h	50	472 ± 59	90	133.2 ± 16.3
G	PVAm	12.5	1 h	50	414 ± 119	88	76.7 ± 9.8
H	Control (water + dioxane)		1 h	60	428 ± 68	N/D	0.3 ± 0.1
I	Control (water + dioxane)		1 h	50	420 ± 85	85	0.4 ± 0.1
J			10 min	50		78	0.3 ± 0.1
K	EtDA		20 min	50		82	0.4 ± 0.1
L			30 min	50		83	0.3 ± 0.1
M	Control (MeOH only)		20 min	50		86	0.2 ± 0.1

N/A: Not Applicable. The mats were too fragile for accurate Orange II measurements.

N/D: Not Determined.

The porosity values were only calculated for the mats that were used in cellular assays, i.e., mats treated at 50°C. These values correspond to the average of measurements performed on 3 distinct mats. Based on the precision of the procedure, we estimate that the standard deviation of these values is about 2%.

not significantly higher than for negative control (condition M, Table 1: pristine samples immersed in MeOH only, $0.2 \pm 0.1 \mu\text{mol/g}$). Even though AFD and mat porosity were not significantly altered by the treatment, it should be noted that a large degradation of the PLA mats was observed after EtDA-based aminolysis starting from 10 min, as revealed by very poor mechanical properties (data not shown).

EGF grafting on aminated PLA mats

NHS ester functionalized homobifunctional PEG linker (Bis(NHS)PEG₅) was used to chemically graft recombinant human EGF onto PAAm-aminolysed mats. rhEGF grafting was evaluated via direct enzyme-linked immunosorbent assay (ELISA, Fig. 3). The NHS functionality of the PEG linker was first reacted with the surface-exposed amine groups to create stable amide bonds. Remaining NHS groups were then used to couple rhEGF via its available amino groups. After EGF grafting, an ethanolamine-mediated NHS deactivation was applied to prevent undesired attachment of other molecules containing amino groups, such as the secondary antibodies used in the ELISA. The growth factor coating was characterized by an ELISA-like method, in which resulting optical density (O.D.) is directly related to the amount of grafted EGF, as previously demonstrated.²⁷ EGF-grafted samples showed an O.D. value of 0.774 ± 0.062 A.U. (condition a on Fig. 3) which was significantly different from the negative controls (condition b and c on Fig. 3). Note that those 2 controls showed non-significant variations in O.D. values, suggesting

that the non-specific adsorption of EGF was negligible. Furthermore, another negative control was performed with aminated mats only. An even lower value (0.033 ± 0.0007 A.U.) was observed compared to the ethanolamine-deactivated PEG layers. Altogether, these results indicated that EGF was covalently attached thanks to the linker with negligible adsorption.

Cell proliferation assays

NSLCs were seeded and cultivated on different PLA scaffolds for 14 d, while changing the media every 2 d. EGF-grafted PLA mats were compared with their negative controls, namely pristine and aminated mats. To differentiate the bioactivity of grafted EGF from that of soluble growth factors supplemented in the medium (i.e., soluble EGF and FGF), different media formulations were used: growth factor-free medium (referred to as 'basal'), EGF-free medium (with soluble FGF) and full medium (with both soluble FGF and EGF). As positive control, NSLC proliferation was also characterized on laminin-coated mats in EGF-free medium.

When grown in basal medium, the number of NSLCs was significantly higher ($p < 0.05$ as determined by 2-way ANOVA) on EGF-grafted mats than on aminated scaffolds or pristine scaffolds (Fig. 4). These results indicated that randomly grafted EGF remained at least partly bioactive, in spite of already documented negative impacts of the random amine coupling strategy²⁸ and still showed its well-known effect on proliferation.^{5,29} Similarly, when grown in EGF-free medium, NSLC proliferation was also

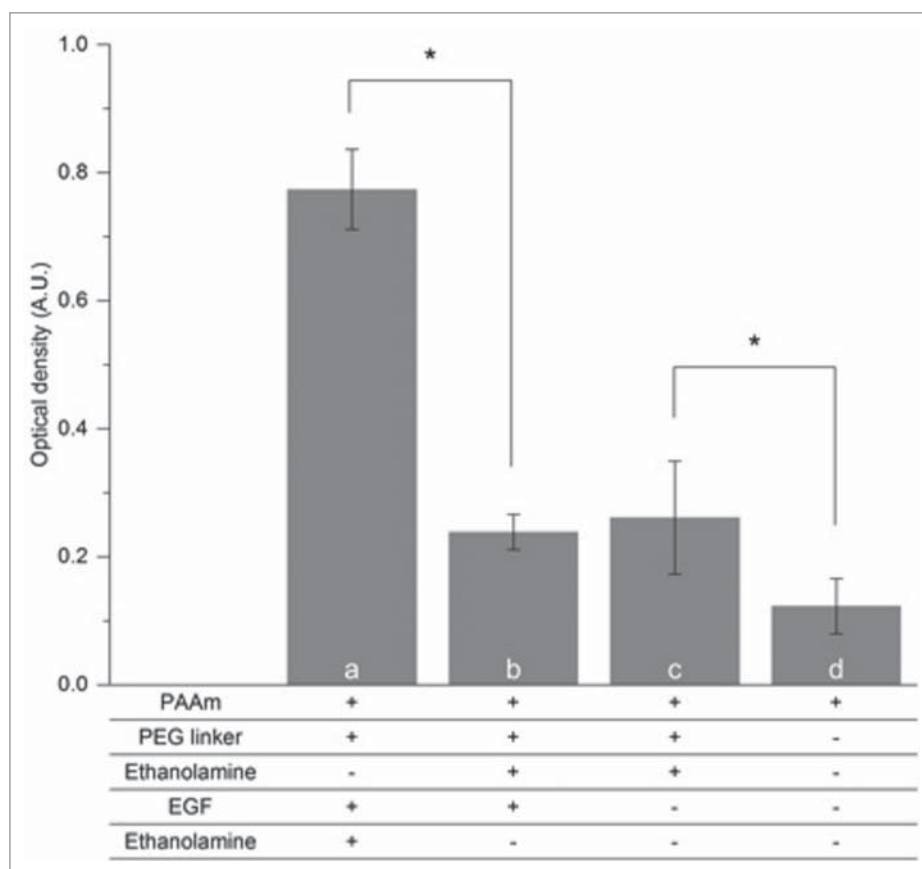


Figure 3. Characterization of the EGF grafting on PLA nanofibers by direct ELISA ($n = 4$). Optical densities (O.D.) corresponding to PAAm-covered mats treated with (A) PEG linker, EGF and ethanolamine (for deactivation of unreacted PEG), (B) Mats covered with PEG linkers that were deactivated before EGF incubation (C) or without any EGF incubation (D) were used as negative controls. As reference, the O.D. value obtained on (D) unmodified PAAm-covered mats is presented. Statistical differences are noted * ($p < 0.05$).

significantly higher ($p < 0.05$) on EGF-grafted mats than on aminated scaffolds (Fig. 4).

Interestingly, NSLCs were able to proliferate in a similar fashion on EGF-grafted mats in basal medium and EGF-free medium, *i.e.*, up to 18450 ± 3480 and 16550 ± 3060 cells at day 10. In contrast, NSLCs remained very few on aminated mats even at day 10, regardless of the presence of growth factors. No significant differences were observed between the EGF-grafted mats in EGF-free medium, basal medium and the positive control (laminin-coated mats in EGF-free medium).

Representative fluorescent images taken at day 10 confirmed the high cell density observed on EGF-grafted mats, regardless of the medium (Fig. 5, E to G). An abundance of cell clusters was observed on pristine and aminated mats in full medium (Fig. 5B and D), suggesting that untreated PLA scaffolds were not optimal to grow NSLCs. In stark contrast, cell distribution appeared quite homogeneous on EGF-treated mats in basal media and EGF-free medium, although a few

small clusters were noticeable when cultured in full media (Fig. 5G, arrows). Furthermore, even the positive control, *i.e.*, laminin-coated mats, appeared to have cells less spread out compared to EGF-grafted mats.

Immunostaining was performed on NSLCs that were grown on EGF-grafted scaffolds as well as on pristine scaffolds as control, in medium supplemented with FGF only (Fig. 6). β -III tubulin (TUJ-1) positive cells were generated on nanofibers and extended some neurite outgrowth, which indicated that the cells remained viable up to 14 d of culture on both EGF-grafted and pristine mats, although large clusters could again be observed on pristine mats. Expression of nestin, the marker for undifferentiated NSLCs, was also used to investigate the overall impact of fiber topology on loss of stemness. NSLCs remained nestin positive. Together with the small neurite extensions visible for both experimental conditions as well as the lack of large cellular network, it indicated that the cells remained multipotent.

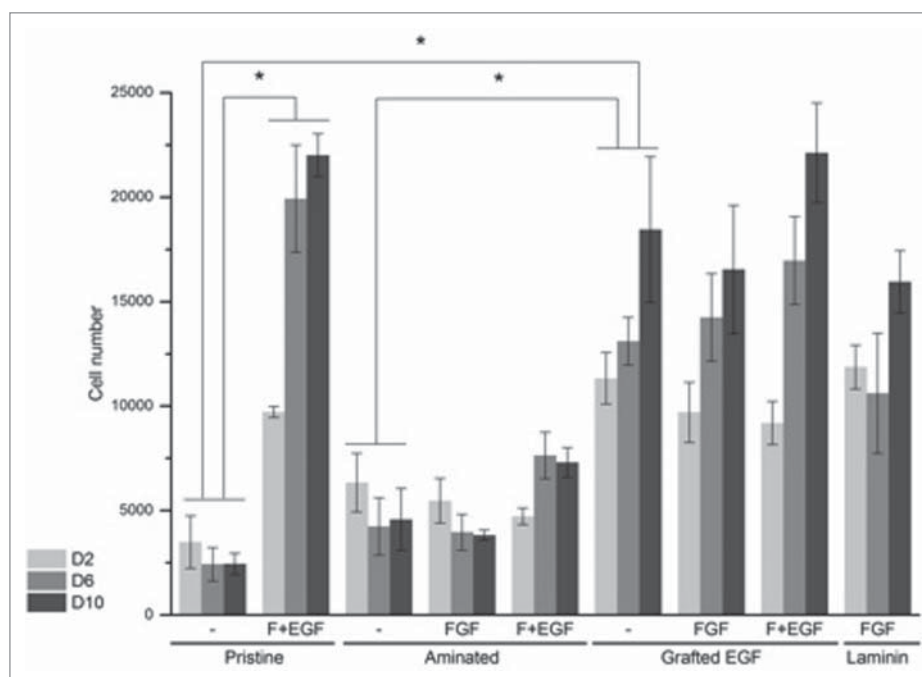


Figure 4. NSLC proliferation on pristine, PAAm-grafted, EGF-grafted and laminin-coated PLA mats ($n = 3$). Cells were cultured in basal medium (denoted "-") or basal medium supplemented with FGF only (denoted FGF) or a mix of FGF and EGF (denoted F + EGF) for 2 d (D2, light gray), 6 d (D6, medium gray) or 10 d (D10, dark gray). Error bars correspond to standard deviation. Statistical differences noted * correspond to $p < 0.05$.

Discussion

PLA nanofiber mats were produced by electrospinning, as biodegradable and highly porous (about 87%) scaffolds suitable for neural tissue engineering. In order to improve NSLC growth onto these scaffolds, our strategy was to bring reactive moieties onto PLA electrospun mats to subsequently graft relevant cell-signaling molecules, thereby tailoring the PLA scaffold. In order to control the identity and quantity of functional groups, wet chemistry aminolysis was tested as we have successfully applied it to PET amination with PVAm.²¹ The chemical treatment was however adapted by decreasing the initial reaction time and temperature (*i.e.* 24 h at 70°C) to 1 h at 50°C, illustrating the differences in degradability between PET microfibers and PLA nanofibers. In our study, polyallylamine (PAAm) was used instead of PVAm because of their strong similarities (one additional carbon on the side chains of PAAm) and the lower cost of PAAm. The pH was found to be a critical parameter as alkaline conditions are needed for the aminolysis to occur via the unprotonated primary amines of either PVAm or PAAm.²¹ Compared to the commonly used ethylenediamine, the polymer-based aminolysis allowed us to mostly preserve the physical properties

of the electrospun mats, *i.e.*, porosity and fiber diameter, without any noticeable change on SEM images.

An extensive NSLC proliferation study was carried out onto various modified PLA mats in various media. When soluble growth factors were present in the medium, NSLCs were able to proliferate onto pristine PLA mats; however, they tended to form cell clusters (Fig. 5B and D), an indication of their low affinity for the hydrophobic substrate.³⁰⁻³³ The PAAm modification of PLA scaffolds advantageously switched surface properties from hydrophobic to hydrophilic (positively charged). That is, although it was impossible to perform any contact angle measurement on these mats to quantify such a change, the switch from hydrophobic to hydrophilic properties was observed during sample preparation (for instance, mats floated in water prior aminolysis whereas such was not the case after aminolysis).

In spite of this change in the hydrophobicity of the mat, aminated PLA scaffolds showed very low NSLC adhesion and proliferation, with a slower growth than that observed on pristine PLA mats (Fig. 4). Such a behavior has been previously reported on surfaces coated with cationic polymers [34], suggesting that PAAm coating most probably provided the mats with inadequate surface properties such as a high positive

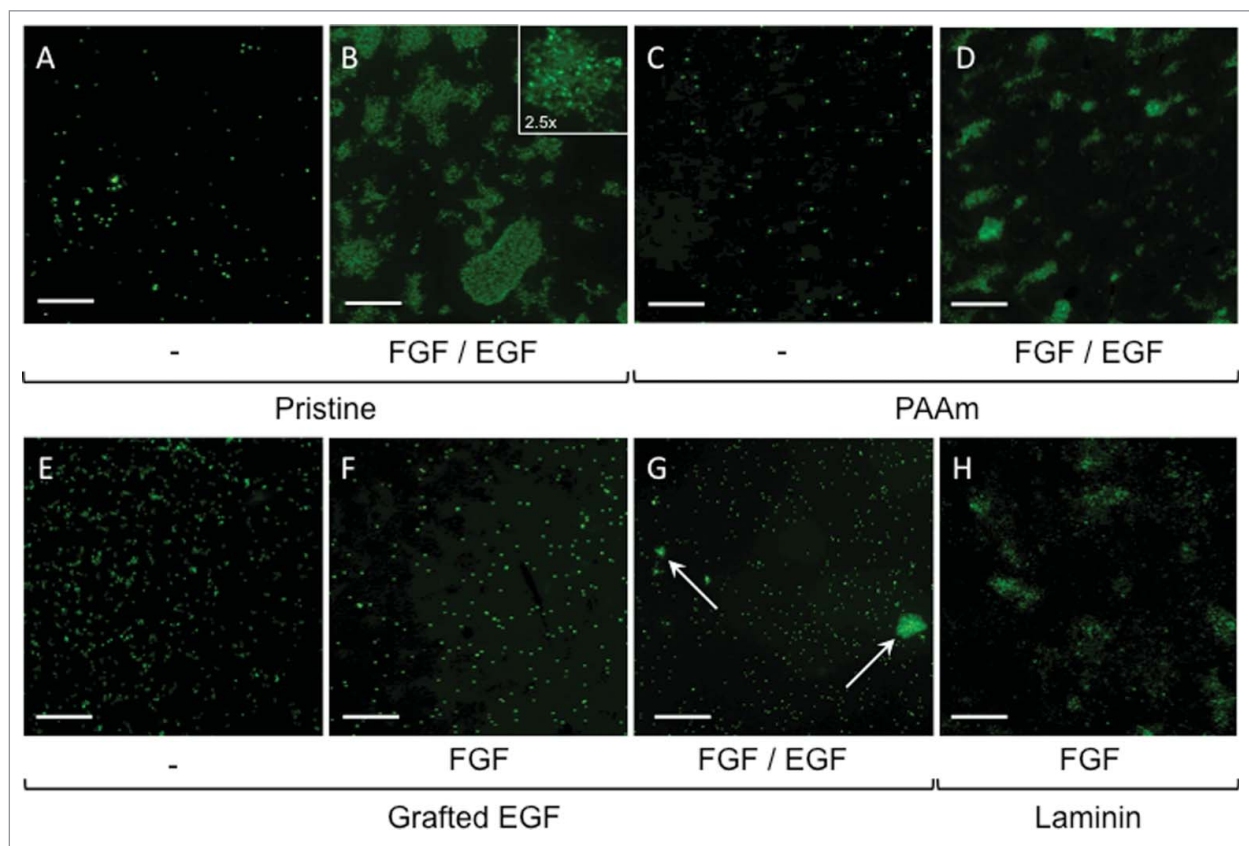


Figure 5. Representative fluorescence imaging (SYTOX) for NSLCs cell proliferation after 10 d of culture on pristine (A, B), PAAm-grafted (C, D), EGF-grafted (E, F, G) and laminin-coated PLA mats (H). Cells were cultured in basal medium (denoted “-”) or basal medium supplemented with FGF only (denoted FGF) or a mix of FGF and EGF (FGF/EGF). Scale bars correspond to 400 μm .

charge and a very high hydrophilicity. Indeed, surfaces with moderate wettability are desirable for good cell adhesion and positive cell response.³⁴⁻³⁷ Coatings that were too hydrophilic were shown to prevent proliferation as well as adhesion of both proteins and cells, such is the case for dense PEG coatings.^{36,38,39} That hypothesis is supported by our data for the first time point of our proliferation study (Fig. 4, day 2), which was mostly representative of adhesion considering that the NSLCs have a doubling time of ca. 37 h. On aminated mats, NSLCs adhesion levels were indeed quite low, regardless of the presence of growth factors in the medium, that is in basal, EGF-free and full media (from 4720 ± 400 to 6340 ± 1400 cells). Cell adhesion being mostly driven by protein adsorption, our results suggest that PAAm-modified mats were indeed protein-repellent, unlike pristine mats onto which cells adhered better in full medium (9720 ± 260 cells) than in basal medium (3490 ± 1260 cells). As stated by others,⁴⁰ PAAm may not prevent cell growth *per se* but could hinder cell spreading and consequently proliferation.

Epidermal growth factor (EGF), that is known to promote cell proliferation, was then grafted onto the available amino groups of PAAm-functionalized PLA mats. A PEG molecule was used as both spacer and chemical linker between PAAm and EGF amino groups. That grafting strategy proved to be both efficient and specific as negligible non-specific adsorption of EGF was observed. That functionalization proved to be beneficial right from cell adhesion, be it in basal medium, EGF-free media or full media (Fig. 4). That additional layer of molecules most probably hid part of the PAAm hydrophilic background, thus promoting cell adhesion in a similar fashion as adsorbed proteins, in addition to providing the cells with a proliferative cue. The bioactivity of grafted EGF *per se* was also demonstrated since NSLCs were able to proliferate on EGF-modified scaffolds at rates similar to our positive control (Fig. 4). The cell remained viable up to day 14 and maintained a multipotent phenotype while in a proliferative state (as evidenced by nestin expression, Fig. 6). Therefore, culturing NSLCs on EGF-grafted nanofibers could be used to maintain the self-renewal and

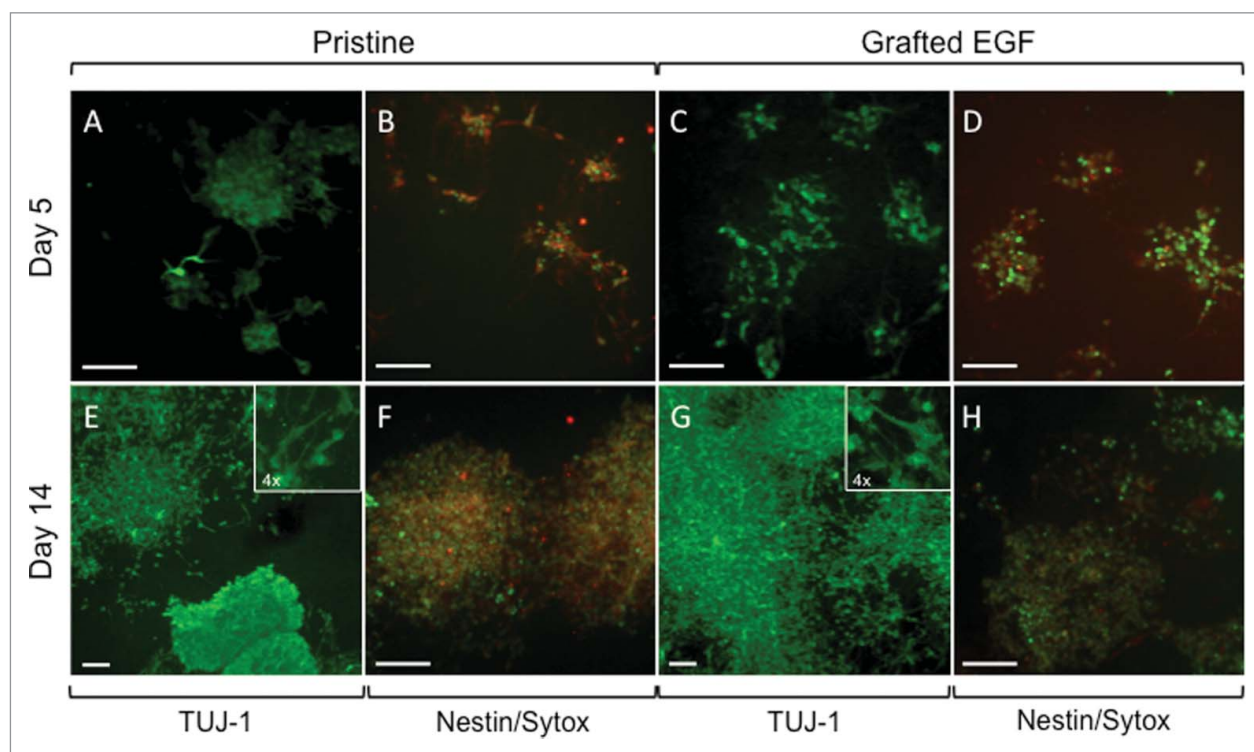


Figure 6. Representative Fluorescent imaging of NSLCs cultured after 5 d (A-D) or 14 d (E-H) of culture on pristine and EGF-grafted mats. Cells were positively stained for β III-Tubulin (A, E, C, G) and nestin (B, F, D, H) under continued proliferation conditions. Cell nuclei were labeled with SYTOX green (B, F, D, H). The scale bars correspond to 100 μ m. When present, insets correspond to a 4x higher magnification of the corresponding image.

stemness of these cells before triggering their differentiation by subsequent addition of specific biological cues.

Conclusion

In this study, we report the successful surface functionalization of poly lactic acid (PLA) electrospun nanofibers with amine groups while maintaining the overall mechanical and structural properties of the scaffold. The scaffold modifications allowed for covalent immobilization of EGF onto PLA fibers in a 2-step process: surface aminolysis followed by conjugation of EGF via a PEG linker. Cell culture studies clearly demonstrated that EGF enhanced cell viability by maintaining pluripotent cells in a proliferative state, which was supported by fluorescence microscopic images.

Materials and methods

Preparation of random PLA nanofibers using electrospinning

The polymer solutions for the fabrication of the nanofibers were prepared by dissolving 2 g of PLA (Cat.# 4032D, NatureWorks LLC, $M_w = 100,000$ g/mol and

polydispersity of 1.75) into a mixture of dichloromethane (DCM, 7 mL; Sigma-Aldrich) and trifluoroacetic acid (TFA, 6 mL; Sigma-Aldrich) to yield a PLA concentration of 15.4% w/v. The polymer solution was placed into a glass syringe (Cadence scientific; needle size 22G) injected at a feeding rate of 0.5 mL/h. A voltage of 23.75 kV was applied. The PLA nanofibers were collected on non-stick aluminum foil at a distance of 10 cm from the needle on a rotating collector (175 rpm).

Nanofiber amination and amine group quantification

The PLA nanofibers were rinsed extensively in ethanol (EtOH, 99.9% purity) and dried in a laminar flow cabinet at room temperature (RT). Three aminolysis procedures were compared and in each case, the amino group quantification was performed by the Orange II method.²² Unless mentioned otherwise, chemical and reagents were obtained from Sigma-Aldrich.

Polyallylamine (PAAm) functionalization

Electrospun PLA were functionalized with PAAm, adapting a protocol for PET aminolysis²¹. An alkaline

solution of NaOH and KCl (1:1, 150 mM in water) and a solution of PAAm (Polysciences Inc.; 85.5 g/L in water) were prepared, and mixed with dioxane (67:7:26% v/v). Prior to dioxane addition, the pH was adjusted to 11.5 or 12.5 by adding few microliters of HCl (12.3 M). The solution was degassed under vacuum for 20 min while stirring. The PLA fibers were immersed in the solution for 1 h at 50°C.

Polyvinylamine (PVAm) functionalization

A solution of PVAm•HCl (Polysciences Inc., 120 g/L in water) was prepared. The PLA fibers were immersed in a degassed mix of the alkaline solution previously described (67:7:26 % v/v) for 1 h at 50°C. The pH of the aqueous solution was set to pH 12.5 prior to dioxane addition.

Ethylenediamine (EtDA) functionalization

The PLA fibers were immersed in a solution of EtDA: MeOH of varying concentrations (0.5, 1, 5, 20 and 30% v/v). The reactions were carried out at 50°C for reaction times set to 10, 20, 30 or 40 min.

Immobilization and quantification of epidermal growth factor (EGF) on nanofibers

EGF grafting on amine-functionalized nanofibers

Aminolysed nanofibers were reacted for 45 min at RT with a freshly prepared solution of Bis-N-succinimidyl-(pentaethylene glycol) ester linker (Bis(NHS)PEG₅, Pierce Biotechnology), *i.e.* 2.5 mM Bis(NHS)PEG₅ in 10 mM phosphate buffer (PBS) containing 1% v/v dimethylsulfoxide (DMSO). The mats were then rinsed in PBS to remove any unbound linker. The PEG-covered nanofibers were then reactivated for 15 min at RT with a 50:50 v:v mixture of N-Hydroxysuccinimide (NHS) (0.1 M in Milli-Q water) and 1-ethyl-3-(3-dimethylaminopropyl) carbodiimide (EDC) (0.4 M in Milli-Q water). After rinsing, the mats were reacted with 100 nM recombinant human EGF (rhEGF, Cat.# 236-EG, R&D systems) in PBS for 1 h at RT and rinsed with PBS. Unreacted NHS groups were blocked using 1 M ethanolamine (pH 8.5) followed by a rinsing step (PBS).

EGF density quantification via Enzyme-Linked Immunosorbent Assay (ELISA)

Quantification of covalently bound EGF was based on previously reported work.²⁷ Commercially available

DuoSet ELISA kit was purchased from Cedarlane (Cat.# DY236). Circular mats (0.785 cm²) were cut, introduced in a 48-well plate and covered with 300 μL of a 1% w/v bovine serum albumin (BSA) solution in PBS (PBS-BSA) for 15 min at RT. After rinsing with a washing solution containing 0.05% Tween 20 diluted in PBS (PBS-T), 300 μL of EGF detection antibody (50 ng/mL in PBS-BSA) were incubated for 1 h at RT. After a second wash with PBS-T, 300 μL of streptavidin-HRP (diluted 200 times with PBS-BSA) were incubated for 20 min at RT. Following a final wash with PBS-T, the reaction was revealed with 300 μL of substrate solution (50:50% v/v hydrogen peroxide/tetramethylbenzidine). After 30 min in the dark, the colorimetric reaction was stopped by adding 150 μL of 2 N H₂SO₄. The supernatants were transferred to a 96-well plate and the optical density at 450 nm was measured.

PLA scaffolds characterization

Structural morphology of PLA scaffolds

The diameters of the fibers were measured from scanning electron microscopy (SEM) photographs using the ImageJ software (NIH, USA). Prior to characterization, the scaffolds were coated with gold (twice for 15 s) using a sputter coater. The porosity and the apparent density were evaluated according to equations 1 and 2:

$$\text{Porosity (\%)} = \left(1 - \frac{\text{apparent density (g / cm}^3\text{)}}{\text{bulk density (g / cm}^3\text{)}} \right) \times 100 \quad (1)$$

$$\begin{aligned} \text{Apparent density (g / cm}^3\text{)} \\ &= \frac{\text{mat mass (g)}}{\text{mat thickness (cm)} \times \text{mat area (cm}^2\text{)}} \quad (2) \end{aligned}$$

where the bulk density of pure PLA is 1.25 g/cm³.⁴¹ Mat dimensions (area and thickness) were measured along each sample and the average values were used for calculations. Weight was recorded for each sample.

Neural stem cell assays

Cell culture

Engineered Neural Stem-Like Cells (NSLC) provided by New World Laboratories Inc. (Laval, QC) were cultured in a medium prepared by mixing neural progenitor basal medium (NPBM, Cedarlane, Cat.# 3210) with neural progenitor supplement singlequote kit

(Cedarlane, Cat.# 4242) and neural progenitor maintenance medium (NPMM) singlequot kit. The NPMM kit contained recombinant human (rh) EGF and FGF (Cedarlane, Cat.# 4241) supplied in a sterile buffered BSA saline solution; 0.1 ml of rhEGF and rhFGF were used for cell seeding medium. Laminin was also added as supplement (5 mg/L) for cell culture. The cells were cultivated in flasks at 37°C with 5% CO₂ in complete maintenance medium. Cells were always used between passage 10 and 14.

Prior to *in vitro* culture, the nanofiber mats were cut into 1-cm diameter disks and exposed to UV for 30 min for sterilization. The samples were then placed into 48-well plates (VWR, Cat.# 82050-888) under a sterile laminar hood. Autoclaved glass cylinders (8-mm inner diameter) were placed onto the samples. To improve cell attachment, samples were coated with laminin (20 µg/mL) in PBS for 1 h and then gently washed 3 times with PBS.

For cell seeding, 1 ml of cell suspension at a cell density of 1.6×10^4 cells was loaded on the top of the nanofibers. The medium (2 mL) was replenished every other day. The cells were incubated within either growth factor-free medium (referred to as 'basal medium'), basal medium + soluble FGF (referred to as 'EGF-free medium'), or basal medium + soluble FGF + soluble EGF (referred to as 'full medium') and incubated at 37°C, 5% CO₂ for 2 weeks.

Proliferation assays. The cell counts on the nanofibers were examined as a function of culture time (2, 6 and 10 days) to assess adhesion and growth. At the specified time point, the cell-seeded samples were first washed with PBS 3 times and fixed in a formaldehyde solution (3.75% w/v in PBS) for 30 min in an incubator. After three PBS washes, the cells were stained with SYTOX Green Nucleic Acid Stain (1 µM in PBS; 300 µL per well; Invitrogen, Cat.# S7020) for 15 min in the dark then washed again 3 times. The stained samples were visualized under a fluorescent microscope and images of complete samples were captured. Cells were counted on SYTOX stained images with the ImageJ software, for 4 different samples per group.

Phenotype analysis. Cells were fixed with 4% paraformaldehyde at 40°C for 30 min and then permeabilized and blocked with 1x PBS containing Triton (0.5% v/v, 20 min). The blocking step was performed using normal donkey serum (NDS) in PBS (Sigma, Cat.#

D9663-10 ML) for 1 h at 5% v/v and 2 h at 10% v/v prior to nestin and β-III-tubulin (TUJ-1) immunostaining, respectively. Samples were immunostained at 4°C overnight with different primary antibodies: goat anti-nestin (undifferentiated neural stem cell marker, Santa Cruz Biotech, Cat.# sc-21248) or mouse anti-TUJ-1 (immature neuron marker, Neuromics, Cat.# MO15013). Primary antibodies were diluted to 3 µg/mL in 0.1% v/v Triton, 1% v/v NDS in PBS. After 3 additional washes, samples were incubated with secondary antibodies: donkey anti-goat or goat anti-mouse (Santa Cruz Biotech, Cat.# sc-362265 and sc-362257, respectively) in 1% v/v NDS for nestin stained samples and in 8% v/v NDS for TUJ-1 stained samples. After a 1 h incubation, cells were washed with a Tween solution (0.1% v/v in PBS) 3 times for 5 min. At the end, SYTOX green was added during 15 min at 1 µM to stain nuclei, as for proliferation assays. The stained samples were visualized under fluorescent microscope.

Statistical analysis

All quantitative data are expressed as means ± standard deviations of a representative experiment performed in *n* replicates, as specified in figure captions. Statistical analysis was performed with one-way analysis of variance (ANOVA) except for the proliferation assays where 2-way ANOVA was used, one factor being the conditions (surface and medium) and the other being time. All ANOVA were followed by a Bonferroni post-hoc test for means comparison. Data sets were considered significantly different from one another for p-values below 0.05 (denoted as * in figures).

Disclosure of potential conflicts of interest

This work was financially supported by New World Laboratories Inc.

Acknowledgements

Authors would like to thank Loïc Binan for help during this work.

Funding

This work was supported by a Research and Development Collaborative grant from the Natural Sciences and Engineering Research Council of Canada (A.A., G.DC) and New World Laboratories Inc., as well as by the Canada Research Chair on Protein-enhanced Biomaterials (G.DC).

ORCID

Gregory De Crescenzo  <http://orcid.org/0000-0002-6280-1570>

References

- [1] Cummings BJ, Uchida N, Tamaki SJ, Salazar DL, Hooshmand M, Summers R, Gage FH, Anderson AJ. Human neural stem cells differentiate and promote locomotor recovery in spinal cord-injured mice. *Proc Natl Acad Sci USA* 2005; 102:14069-74; PMID:16172374; <http://dx.doi.org/10.1073/pnas.0507063102>
- [2] Akesson E, Sandelin M, Kanaykina N, Aldskogius H, Kozlova EN. Long-term survival, robust neuronal differentiation, and extensive migration of human forebrain stem/progenitor cells transplanted to the adult rat dorsal root ganglion cavity. *Cell Transplant* 2008; 17:1115-23; PMID:19181206; <http://dx.doi.org/10.3727/096368908787236585>
- [3] Parr AM, Kulbatski I, Zahir T, Wang X, Yue C, Keating A, Tator CH. Transplanted adult spinal cord-derived neural stem/progenitor cells promote early functional recovery after rat spinal cord injury. *Neuroscience* 2008; 155:760-70; PMID:18588947; <http://dx.doi.org/10.1016/j.neuroscience.2008.05.042>
- [4] Nakaji-Hirabayashi T, Kato K, Arima Y, Iwata H. Oriented immobilization of epidermal growth factor onto culture substrates for the selective expansion of neural stem cells. *Biomaterials* 2007; 28:3517-29; PMID:17482256; <http://dx.doi.org/10.1016/j.biomaterials.2007.04.022>
- [5] Tropepe V, Sibilia M, Ciruna BG, Rossant J, Wagner EF, van der Kooy D. Distinct Neural Stem Cells proliferate in response to EGF and FGF in the developing mouse telencephalon. *Dev Biol* 1999; 208:166-88; PMID:10075850; <http://dx.doi.org/10.1006/dbio.1998.9192>
- [6] Karimi-Abdolrezaee S, Eftekharpour E, Wang J, Morshead CM, Fehlings MG. Delayed transplantation of adult neural precursor cells promotes remyelination and functional neurological recovery after spinal cord injury. *J Neurosci* 2006; 26:3377-89; PMID:16571744; <http://dx.doi.org/10.1523/JNEUROSCI.4184-05.2006>
- [7] Jezierski A, Rennie K, Zurakowski B, Ribocco-Lutkiewicz M, Haukenfrers J, Aji A, Gruslin A, Sikorska M, Bani-Yaghoob M. Neuroprotective effects of GDNF-expressing human amniotic fluid cells. *Stem Cell Rev* 2014; 10:251-68; PMID:24415130; <http://dx.doi.org/10.1007/s12015-013-9484-x>
- [8] Guo X, Zahir T, Mothe A, Shoichet MS, Morshead CM, Katayama Y, Tator CH. The effect of growth factors and soluble Nogo-66 receptor protein on transplanted neural stem/progenitor survival and axonal regeneration after complete transection of rat spinal cord. *Cell Transplant* 2012; 21:1177-97; PMID:22236767; <http://dx.doi.org/10.3727/096368911X612503>
- [9] Subramanian A, Krishnan UM, Sethuraman S. Development of biomaterial scaffold for nerve tissue engineering: Biomaterial mediated neural regeneration. *J Biomed Sci* 2009; 16:108; PMID:19939265; <http://dx.doi.org/10.1186/1423-0127-16-108>
- [10] Tayalia P, Mooney DJ. Controlled Growth Factor Delivery for Tissue Engineering. *Adv Mater* 2009; 21:3269-85; PMID:20882497; <http://dx.doi.org/10.1002/adma.200900241>
- [11] Peppas NA, Hilt JZ, Khademhosseini A, Langer R. Hydrogels in biology and medicine: From molecular principles to bionanotechnology. *Adv Mater* 2006; 18:1345-60; <http://dx.doi.org/10.1002/adma.200501612>
- [12] Zuidema JM, Pap MM, Jaroch DB, Morrison FA, Gilbert RJ. Fabrication and characterization of tunable polysaccharide hydrogel blends for neural repair. *Acta Biomater* 2011; 7:1634-43; PMID:21130187; <http://dx.doi.org/10.1016/j.actbio.2010.11.039>
- [13] Wang Y, Wei YT, Zu ZH, Ju RK, Guo MY, Wang XM, Xu QY, Cui FZ. Combination of hyaluronic acid hydrogel scaffold and PLGA microspheres for supporting survival of neural stem cells. *Pharm Res* 2011; 28:1406-14; PMID:21537876; <http://dx.doi.org/10.1007/s11095-011-0452-3>
- [14] Yang F, Murugan R, Wang S, Ramakrishna S. Electrospinning of nano/micro scale poly(L-lactic acid) aligned fibers and their potential in neural tissue engineering. *Biomaterials* 2005; 26:2603-10; PMID:15585263; <http://dx.doi.org/10.1016/j.biomaterials.2004.06.051>
- [15] Yang F, Xu CY, Kotaki M, Wang S, Ramakrishna S. Characterization of neural stem cells on electrospun poly(L-lactic acid) nanofibrous scaffold. *J Biomater Sci Polym Ed* 2004; 15:1483-97; PMID:15696794; <http://dx.doi.org/10.1163/1568562042459733>
- [16] Pham QP, Sharma U, Mikos AG. Electrospinning of polymeric nanofibers for tissue engineering applications: A review. *Tissue Eng* 2006; 12:1197-211; PMID:16771634; <http://dx.doi.org/10.1089/ten.2006.12.1197>
- [17] Xu CY, Inai R, Kotaki M, Ramakrishna S. Aligned biodegradable nanofibrous structure: a potential scaffold for blood vessel engineering. *Biomaterials* 2004; 25:877-86; PMID:14609676; [http://dx.doi.org/10.1016/S0142-9612\(03\)00593-3](http://dx.doi.org/10.1016/S0142-9612(03)00593-3)
- [18] Fadeev AY, McCarthy TJ. Surface modification of poly(ethylene terephthalate) to prepare surfaces with silica-like reactivity. *Langmuir* 1998; 14:5586-93; <http://dx.doi.org/10.1021/la980512f>
- [19] Yang P, Zhang X, Yang B, Zhao H, Chen J, Yang W. Facile preparation of a patterned, aminated polymer surface by UV-light-induces surface aminolysis. *Adv Funct Mater* 2005; 15:1415-25; <http://dx.doi.org/10.1002/adfm.2004-00335>
- [20] Dimitrievska S, Maire M, Diaz-Quijada GA, Robitaille L, Aji A, Yahia L, Moreno M, Merhi Y, Bureau MN. Low thrombogenicity coating of nonwoven PET fiber structures for vascular grafts. *Macromol Biosci* 2011; 11:493-502; PMID:21259437; <http://dx.doi.org/10.1002/mabi.201000390>
- [21] Noel S, Liberelle B, Yogi A, Moreno MJ, Bureau MN, Robitaille L, De Crescenzo G. A non-damaging chemical amination protocol for poly(ethylene terephthalate) -

- application to the design of functionalized compliant vascular grafts. *J Mater Chem B* 2013; 1:230-8; <http://dx.doi.org/10.1039/C2TB00082B>
- [22] Noel S, Liberelle B, Robitaille L, De Crescenzo G. Quantification of primary amine groups available for subsequent bio-functionalization of polymer surfaces. *Bioconjugate Chem* 2011; 22:1690-9; <http://dx.doi.org/10.1021/bc200259c>
- [23] Ahlfors JE, Elayoubi R. *Methods for Reprogramming Cells and Uses Thereof*. US20120220034 A1 2012.
- [24] Jamshidi K, Hyon S-H, Okada Y. Thermal characterization of polylactides. *Polymer* 1988; 29:2229-34; [http://dx.doi.org/10.1016/0032-3861\(88\)90116-4](http://dx.doi.org/10.1016/0032-3861(88)90116-4)
- [25] Ishiyama C, Higo Y. Effects of humidity on Young's modulus in poly(methylmethacrylate). *J Polym Sci, Part B: Polym Phys* 2002; 40:460-5; <http://dx.doi.org/10.1002/polb.10107>
- [26] Shen J, Chen CC, Sauer JA. Effects of sorbed water on properties of low and high molecular weight PMMA: 1. Deformation and fracture behaviour. *Polymer* 1985; 26:511-8; [http://dx.doi.org/10.1016/0032-3861\(85\)90150-8](http://dx.doi.org/10.1016/0032-3861(85)90150-8)
- [27] Lequoy P, Liberelle B, De Crescenzo G, Lerouge S. Additive benefits of chondroitin sulfate and oriented tethered epidermal growth factor for vascular smooth muscle cell survival. *Macromol Biosci* 2014; 14:720-30; PMID:24469944; <http://dx.doi.org/10.1002/mabi.201300443>
- [28] Liberelle B, Boucher C, Chen JK, Jolicoeur M, Durocher Y, De Crescenzo G. Impact of Epidermal Growth Factor Tethering Strategy on Cellular Response. *Bioconjugate Chem* 2010; 21:2257-66; <http://dx.doi.org/10.1021/bc1002604>
- [29] Cooke MJ, Wang Y, Morshead CM, Shoichet MS. Controlled epi-cortical delivery of epidermal growth factor for the stimulation of endogenous neural stem cell proliferation in stroke-injured brain. *Biomaterials* 2011; 32:5688-97; PMID:21550655; <http://dx.doi.org/10.1016/j.biomaterials.2011.04.032>
- [30] Jeon O, Alsberg E. Regulation of stem cell fate in a three-dimensional micropatterned dual-crosslinked hydrogel system. *Adv Funct Mater* 2013; 23:4765-75; PMID:24578678
- [31] Nelson CM, Chen CS. Cell-cell signaling by direct contact increases cell proliferation via a PI3K-dependent signal. *FEBS Lett* 2002; 514:238-42; PMID:11943158; [http://dx.doi.org/10.1016/S0014-5793\(02\)02370-0](http://dx.doi.org/10.1016/S0014-5793(02)02370-0)
- [32] Liu WF, Nelson CM, Pirone DM, Chen CS. E-cadherin engagement stimulates proliferation via Rac1. *J Cell Biol* 2006; 173:431-41; PMID:16682529; <http://dx.doi.org/10.1083/jcb.200510087>
- [33] Johnson WE, Eisenstein SM, Roberts S. Cell cluster formation in degenerate lumbar intervertebral discs is associated with increased disc cell proliferation. *Connect Tissue Res* 2001; 42:197-207; PMID:11913491; <http://dx.doi.org/10.3109/03008200109005650>
- [34] Horbett TA, Schway MB, Ratner BD. Hydrophilic-hydrophobic copolymers as cell substrates: Effect on 3T3 cell growth rates. *J Colloid Interf Sci* 1985; 104:28-39; [http://dx.doi.org/10.1016/0021-9797\(85\)90006-2](http://dx.doi.org/10.1016/0021-9797(85)90006-2)
- [35] Lee JH, Khang G, Lee JW, Lee HB. Interaction of different types of cells on polymer surfaces with wettability gradient. *J Colloid Interface Sci* 1998; 205:323-30; PMID:9735195; <http://dx.doi.org/10.1006/jcis.1998.5688>
- [36] van Wachem PB, Beugeling T, Feijen J, Bantjes A, Detmers JP, van Aken WG. Interaction of cultured human endothelial cells with polymeric surfaces of different wettabilities. *Biomaterials* 1985; 6:403-8; PMID:4084642; [http://dx.doi.org/10.1016/0142-9612\(85\)90101-2](http://dx.doi.org/10.1016/0142-9612(85)90101-2)
- [37] van Wachem PB, Hogt AH, Beugeling T, Feijen J, Bantjes A, Detmers JP, van Aken WG. Adhesion of cultured human-endothelial cells onto methacrylate polymers with varying surface wettability and charge. *Biomaterials* 1987; 8:323-8; PMID:3676418; [http://dx.doi.org/10.1016/0142-9612\(87\)90001-9](http://dx.doi.org/10.1016/0142-9612(87)90001-9)
- [38] Ma ZW, Mao ZW, Gao CY. Surface modification and property analysis of biomedical polymers used for tissue engineering. *Colloids Surf, B* 2007; 60:137-57; <http://dx.doi.org/10.1016/j.colsurfb.2007.06.019>
- [39] Zhu YB, Gao CY, Liu YX, Shen JC. Endothelial cell functions in vitro cultured on poly(L-lactic acid) membranes modified with different methods. *J Biomed Mater Res A* 2004; 69a:436-43; <http://dx.doi.org/10.1002/jbm.a.30007>
- [40] Chen G, Kawazoe N, Tateishi T. Effects of ECM proteins and cationic polymers on the adhesion and proliferation of rat islet cells. *Open Biotechnol J* 2008; 2:133-7; <http://dx.doi.org/10.2174/1874070700802010133>
- [41] Xiao H, Lu W, Yeh JT. Crystallization behavior of fully biodegradable poly(lactic acid)/poly(butylene adipate-*c*-terephthalate) blends. *J Appl Polym Sci* 2009; 112:3754-63; <http://dx.doi.org/10.1002/app.29800>